

# ELECTROTHERMALLY BONDED CARBON NANOTUBE INTERFACES

Sriharsha V. Aradhya, Suresh V. Garimella, Timothy S. Fisher\*  
School of Mechanical Engineering and Birck Nanotechnology Center  
Purdue University  
West Lafayette, Indiana 47907 USA  
Phone: (765) 494-5627, Fax: 765-494-0539  
\*Email: [tsfisher@purdue.edu](mailto:tsfisher@purdue.edu)

## ABSTRACT

Applications that exploit the exceptional transport properties of carbon nanotubes (CNTs) at practical length scales almost invariably require good contact of the CNTs with the contacting surface. For example, vertically aligned and dense arrays of carbon nanotubes have been demonstrated to be good thermal interface materials. However, interfacial resistance to thermal and electrical transport between CNTs and bulk substrates is found to adversely affect device performance in such applications. In this work, we present a method to attach CNTs to contacting surfaces with low-temperature electrostatic bonding, and the effects of bonding conditions are studied in terms of the resulting interface morphology, mechanical bond strength, and thermal conductance. We show that the bonding process results in thermal resistance reductions of as much as 64% compared to unbonded CNT joints. Optimization of such bonded interfaces can lead to utilization of CNT interfaces closer to their full potential.

**Keywords:** thermal interface, carbon nanotubes (CNTs), bonding, contact resistance, electronics cooling

## NOMENCLATURE

$A$	area ( $\text{m}^2$ )
$G$	temperature gradient ( $\text{K/m}$ )
$i$	index
$k$	thermal conductivity ( $\text{W/mK}$ )
$q$	heat flux ( $\text{W}$ )
$R$	thermal resistance ( $\text{mm}^2\text{K/W}$ )
$t$	thickness ( $\text{m}$ )
$T$	temperature ( $\text{K}$ )
$X$	arbitrary measured variable

## Greek symbols

$\delta$	differential
$\Delta$	difference
$\varepsilon$	emissivity

## Subscripts

1, 2	copper bars on top and bottom, respectively
<i>CNT</i>	carbon nanotube array
<i>control</i>	control experiment with bare silicon wafer
<i>Cu</i>	copper
<i>fitted</i>	linear fit of the temperature profile
<i>free tip</i>	exposed carbon nanotube tips contacting a surface
<i>glass</i>	glass
<i>Si</i>	silicon
<i>Sub</i>	growth substrate

*total* full thermal resistance stack

## INTRODUCTION

Thermal technologies for electronics cooling applications are predicted to be increasingly important in the near future [1]. With continual increases in the power dissipation of electronic devices, all aspects of the thermal solution need to be optimized for more efficient cooling. Thermal interface materials are ubiquitous components of cooling solutions [2]. In fact, typical thermal architectures employ multiple thermal interface materials and complement a broad variety of active heat dissipation technologies [3].

Carbon nanotubes (CNTs) have generated tremendous interest in the past decade because of their excellent physical and chemical properties [4]. In particular, individual multi-wall CNTs can have high thermal conductivities of up to 3000 W/mK [5, 6]. However, thermal resistance at the contacts of the CNT array on either side is one of the major factors that has limited the commercial application of CNTs as interface materials. The contact of free tips of CNTs to a surface is typically due to weak van der Waals interactions [7] that impede carrier transport in nanoscale devices and systems. Therefore stronger forces of interaction are needed to replace this weak interaction for effective transport at nanotube contacts.

Thermal transport in suspensions containing carbon nanotubes has been shown by Huxtable *et al.* [8] to be severely limited by interfacial resistance. Using a transient absorption measurement in stable suspensions of carbon nanotubes, they have concluded that transport across the nanotube-surfactant interface is not a strong function of the surfactant itself, but a function of the coupling of phonon vibration modes. A related molecular dynamics simulation study [9] has also shown that this high resistance is due to the absence of covalent bonding that would couple the high frequency phonon states.

A tremendous interest also exists in using CNTs as ballistic transport channels for electronic transistor [10] and for interconnect applications [11]. Contact resistance has been shown to be important [12] in these applications as well. For improving mechanical contacts between vertically aligned carbon nanotube arrays and metals, Zhao *et al.* [7] have used a pre-stressing technique of applying loads on the order of 200 kPa and for a 4 mm<sup>2</sup> area of the CNT array they obtained pull-off forces of about 120 kPa. They reported a strong dependence on the bonded area, with the pull-off force

decreasing to approximately 20 kPa for samples with 10mm<sup>2</sup> bonded area.

Cola *et al.* [13] have studied thermal contact resistance with vertically oriented CNT arrays. They have found that among the CNT-to-growth substrate resistance, CNT array resistance and CNT tip-to-contacting surface resistance present in the thermal interface resistance, the contacting nanotube tip resistance dominated the overall resistance. Further, the large resistance at the free nanotube to surface contact was likely caused by phonon ballistic resistance, given the contact length scales of order 1-10 nm [14]. In the present work, we concentrate on enhancing the interaction between the carbon nanotubes and the contact surface.

### EXPERIMENT

Figure 1 shows a typical vertically oriented CNT array grown by microwave plasma chemical vapor deposition (MPCVD) using a tri-layer catalyst [15] of 30 nm Ti, 10 nm Al and 3 nm Fe on a Si wafer. After annealing the Si wafer in a nitrogen atmosphere inside the MPCVD, CNT growth occurred at 900°C at a gas flow rate of 50 standard cubic centimeters per minute (sccm) of H<sub>2</sub>, 10 sccm of CH<sub>4</sub> and at 300 W plasma power with no bias voltage. The growth length of CNTs depends on the duration of the process. In this study, samples with CNT lengths of about 35 μm are used.

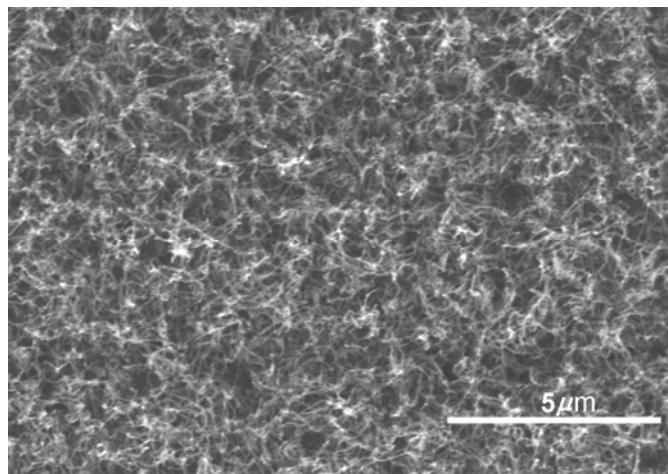


Fig. 1. SEM image (top view) of the surface of an as-grown vertically oriented carbon nanotube array.

### Bonding Process

Anodic bonding is a standard procedure in microfabrication [16]. This process bonds silicon wafers to glass by creating an oxide layer at the interface between silicon and glass [17, 18] and is enabled by the movement of alkali ions, Na<sup>+</sup> or K<sup>+</sup>, depending on the type of glass used. The name of the process is derived from the fact that the alkali ions are driven away from the silicon (anode) surface contacting the glass and toward the cathode terminal of the glass. This ion flow and consequent transfer of charge creates an inversion layer at the anode-cathode interface. The

oppositely charged surfaces are attracted, creating an intimate contact, and oxidation at the interface leads to a strong bond.

We use this migration of alkali ions in a modified protocol to exploit the ability of CNTs to intercalate alkali ions [19] to enable bonding. An objective of the present work is to bond CNT free tips to the contacting surface. We first demonstrate the mechanism by bonding CNT arrays to relatively thick glass slide material. For thermal interface applications, the thickness of the additional glass layer introduced must be minimized because glass is a poor thermal conductor. For such applications, we demonstrate bonding of CNTs to thin-films of glass evaporated on to a silicon wafer.

Figure 2 illustrates the setup used for bonding CNT arrays grown on a silicon growth substrate to a glass slide. The glass slide (Corning Pyrex 7740, thickness 650 microns and area about 5 mm x 5 mm) is connected to the positive terminal, and the Si wafer is connected to the negative terminal of the power supply. The positively charged ions move in the direction opposite to that in conventional anodic bonding, as indicated in Figure 2. A voltage of 1200 V was applied at temperatures between 200°C to 400°C. Bonding was carried out for 30 minutes, and the glass surface was then observed to adhere well to the CNT array. Qualitatively, weaker adhesion was observed for lower temperatures and voltages for the thick glass samples.

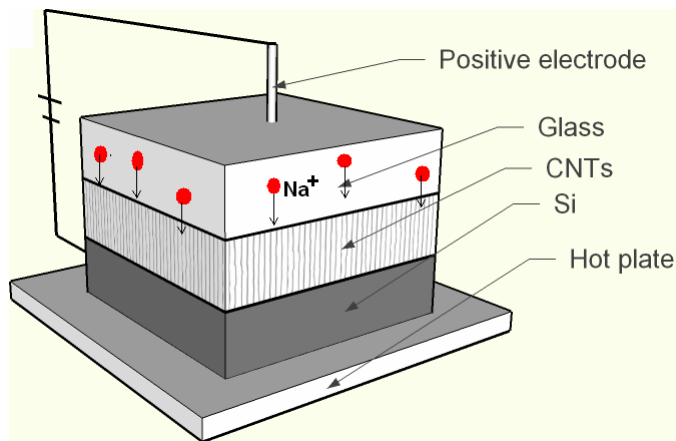


Fig. 2. Schematic of the CNT bonding setup indicating the migration of alkali ions.

For bonding to thin glass films, the glass slide in Figure 2 was replaced by a glass film of thickness 2.5 μm evaporated on to a silicon wafer. The glass film faces the carbon nanotubes, and to maintain the same order of magnitude of bonding current, lower temperatures and voltages were found to be sufficient. Qualitatively, it was observed that good adhesion occurred even at room temperatures, with suitable applied voltages. These more moderate conditions are advantageous because they allow this bonding process to be applied to electronics packaging solutions where high temperatures and voltages can be detrimental to the existing electronic structures.

## Thermal Characterization

Thermal contact resistance is measured in this work using a 1D reference calorimeter (Figure 3) [15]. A top-side cartridge heater (13.5 W power) and a copper block cooled with circulated chilled water at the bottom help maintain the desired heat flux and temperature gradient through the copper bars. The copper bars are 40 mm long and 100 mm<sup>2</sup> in cross section and made from C101 oxygen free high conductivity (OFHC) copper. The copper bar contact surfaces are polished and the external surfaces painted black with Rustoleum black paint ( $\epsilon=0.94$ ). The CNT sandwich (with the silicon growth wafer on one side of the CNT array and the contacting silicon wafer surface on the other) is placed between the two copper bars. The setup has a mechanism for applying pressure on the specimen being measured, and pressures between 0.17 MPa and 0.45 MPa were chosen to span the pressures encountered in electronics cooling applications [2].

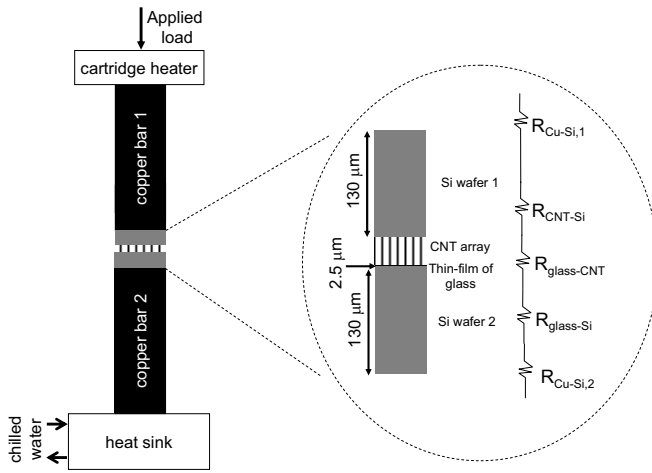


Fig. 3. 1D reference calorimeter setup and expanded view of the thermal resistance stack being measured

The contact resistances at the silicon-copper bar interface are designated  $R_{Cu-Si,1}$  and  $R_{Cu-Si,2}$ . The CNT array is grown on the polished surface of a single-side polished silicon wafer, and the evaporated glass film is deposited on one side of another silicon wafer. The silicon-copper bar thermal interface resistances are first measured from control experiments in which only a single side polished silicon wafer is present instead of the CNT sandwich.  $R_{CNT-Si}$  is the interface resistance between the carbon nanotube array and the silicon growth substrate.  $R_{glass-Si}$  is the interface resistance between the 2.5  $\mu\text{m}$  glass thin film and the polished silicon wafer. We expect  $R_{glass-Si}$  to be small because the glass layer was deposited using electron beam evaporation, which is known to yield conformal coverage of the evaporated material [20].  $R_{glass-CNT}$  is the critical interface resistance of interest between the carbon nanotube array free tips and the thin glass film. Other than these interface resistances, there are also resistances due to silicon ( $R_{Si}$ ) and glass ( $R_{glass}$ ) layers which together contribute about 4 mm<sup>2</sup>K/W to the thermal resistance stack:

$$R_{Si} = t_{Si} / (k_{Si}) \quad (1)$$

$$R_{glass} = t_{glass} / (k_{glass}) \quad (2)$$

An infrared camera (FLIR SC300) is used to measure the temperature profile in the copper bars. The entire setup is in atmosphere. The camera software collects about 100 pixelated temperature measurements over the combined length of the two copper bars. The uncertainty of the temperature measurements is within 0.1°C over a measurement range of -20 to 120°C from calibration with a black body source [15]. This temperature profile is then converted to a temperature gradient ( $G$ ) by linear curve fitting. The gradients for the top and bottom copper bars are within 10% of each other at the 0.17 MPa pressure, and this difference reduces to 5% at the 0.45 MPa pressure. We note that unlike similar prior experiments [15], the experiments were not conducted in vacuum because they were subjected to *in situ* electrothermal bonding during the sequence of thermal measurements, as described below. The average value of  $G$  and area  $A$  of the interface is used to calculate the heat flux ( $q$ ):

$$q = -k_{Cu}AG \quad (3)$$

where  $k_{Cu}$  is the thermal conductivity of copper,  $A$  is the area of the interface (10mm x 10 mm) and  $G$  is the temperature gradient. We neglect heat loss by convection and radiation from the sides of the copper bars in our analysis for the range of temperatures used in this study.

The temperature difference at the interface is estimated by extrapolating the curve-fit temperature profiles of both top and bottom copper bars. The total area-normalized resistance is obtained from the temperature gradient and the calculated heat flux as:

$$R_{total} = R_{Si} + R_{glass} + R_{Cu-Si,1} + R_{Cu-Si,2} + R_{c-Si} + R_{CNT} + R_{glass-Si} \quad (4)$$

$$R_{total} = \Delta T_{fitted} A / q \quad (5)$$

For the control experiments, a similar approach was used, with the total resistance comprising only the resistance of the silicon wafer and the two copper-silicon interfaces:

$$R_{total, control} = R_{Si} + R_{Cu-Si,1} + R_{Cu-Si,2} \quad (6)$$

The measurement uncertainty is influenced by temperature, temperature gradient, area, and other factors [15]. We neglect the variation of thermal conductivity with temperature of the CNTs, copper and silicon because of the relatively small range of temperatures used. From standard theory [21], the uncertainty is calculated as:

$$\delta R = \left[ \sum_i \left( \frac{\partial R}{\partial X_i} \delta X_i \right)^2 + (\delta R_{control})^2 \right]^{1/2} \quad (7)$$

Here  $X_i$  represents  $G$ ,  $\Delta T$ ,  $L$ ,  $A$  or  $k_{Si}$ .  $\delta X_i$  is the uncertainty for each measured quantity  $X_i$ , and  $\delta R$  is the uncertainty in the measured resistance. For the control resistances, the  $\delta R_{control}$  term is absent.

The dominant uncertainty in our experiment is due to the measured temperature gradient. The uncertainty lies between  $\pm 7$  to  $\pm 15$   $\text{mm}^2\text{K/W}$  for the silicon-copper bar control experiments, and between  $\pm 13$  to  $\pm 25$   $\text{mm}^2\text{K/W}$  for the CNT array interface experiments.

We also use the thermal characterization setup for *in situ* bonding during the experiment by applying appropriate polarity to copper bar 1 (cathode) and copper bar 2 (anode). The advantage of this scheme is that it eliminates the large uncertainties that would otherwise arise due to changes in contact conditions if the setup were assembled separately for the bonded and unbonded configurations. Because minimal changes occur in the contact conditions, any measured variations of the thermal resistance upon bonding can be attributed primarily to changes in the carbon nanotube-glass interface.

## RESULTS AND DISCUSSION

Current flow through the specimen undergoing bonding is a direct indication of the overall charge movement. Figure 4a shows the bonding current as a function of time for bonding CNTs to the 650  $\mu\text{m}$  glass slide. The general nature of this plot is typical of a conventional anodic bonding process, with the direction of current reversed. Sodium migration towards the CNT array free-tip surface has been shown to govern this form of current variation [16]. During the bonding of CNTs to the 2.5  $\mu\text{m}$  thin-film of glass evaporated on a silicon surface, we also observe a similar bonding current profile (Figure 4b). A voltage of 100 V at a temperature of 175°C was adequate for this experiment in order to achieve the same order of magnitude of current flow through the specimen as for the glass slide.

The delay of 12 seconds between the time the current is switched on to the peak in its value (inset, Figure 4a) is representative of the total length that the ions have to diffuse. This delay is shorter in the thin film glass interface due to the reduced thickness of glass, despite the reduction in temperature and consequent reduction of diffusivity for the mobile sodium ions. The additional noise in Figure 4b is a manifestation of the unavoidable increase in relative roughness of the glass film deposited by the electron beam evaporation process, evidenced by numerous creasing lines on the evaporated glass surface, as compared to the smooth surface of commercial glass slides.

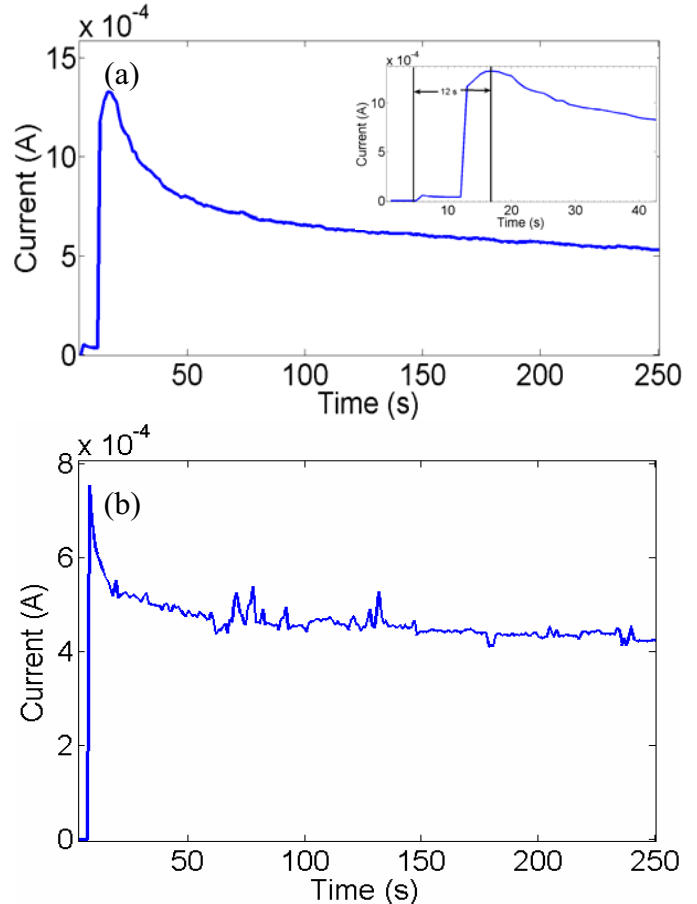


Fig. 4. Bonding current as a function of time for the first 250 seconds of bonding: a) 650  $\mu\text{m}$  glass slide at 400°C with 1000 V (inset: magnified view of the first 40 seconds, showing a 12 second delay between switching on of the current and the peak value), and b) 2.5  $\mu\text{m}$  glass slide at 175°C with 100V.

### Analysis of the Bonding Mechanism

Sodium ion migration during the bonding process is confirmed by analyzing scanning electron micrographs and X-ray photoelectron spectra of the contacting glass slide surface and CNT free tip surface. After carefully separating the CNT array from the glass surface with a razor blade, we visually observe a dark residue remaining on the glass slide surface where the CNT array specimen contacted the glass surface (Figure 5a). This residue is determined to be CNTs that remain adhered to the glass surface after separation of the CNT array, as seen in Figure 5b. The CNT adhesion in the case of the 2.5  $\mu\text{m}$  glass thin-film can be directly observed through SEM imaging (Figure 5c).

Mechanical bonding strength is an important quantity of interest in bonded joints. We perform a pull-test by first bonding a CNT array sample to the 650  $\mu\text{m}$  glass slide at 200°C with a 1000 V applied voltage. The back surface of the silicon wafer is glued to a cantilever, and the back surface of the glass slide is glued to a flat, rigid surface. The force needed to separate the CNT array surface from the glass surface is measured to be 1.2 N. It was observed that CNTs were well-anchored to the growth substrate, but some CNTs

adhered to the glass surface, as described before, indicating that the measured pull-off force can be attributed to interfacial adhesion. Considering the ‘bonding affected area’ to be the area where the CNT residue remained (5.3 mm x 5.2 mm), we estimate a force of about 40 kPa for this bonded interface. This bonding force is significant considering work by Zhao *et al.* [7], who reported forces of this order of magnitude with smaller samples, shorter carbon nanotubes and an order of magnitude higher applied pressure, all three being factors that were identified to enhance adhesive forces in their study.

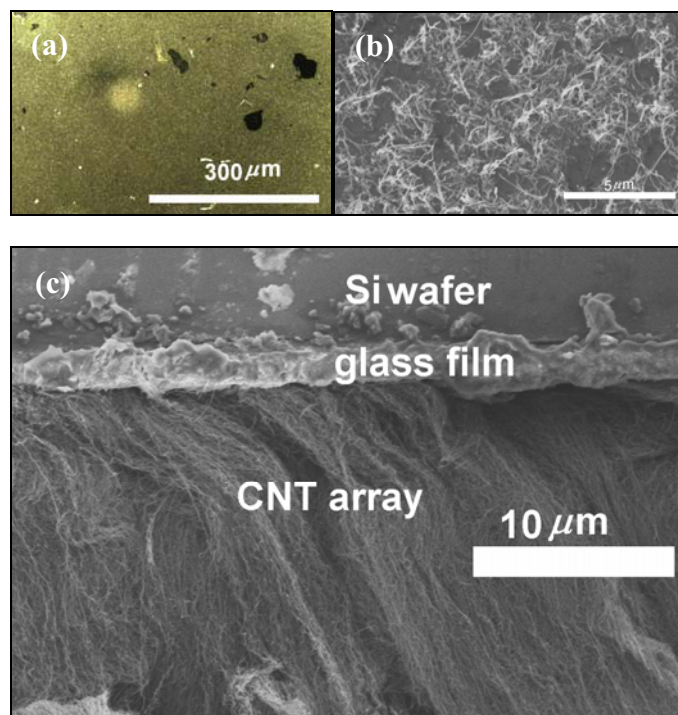


Fig. 5. a) Optical microscope images of the 650  $\mu\text{m}$  glass slide surface b) SEM image showing residual CNTs on the surface of the 650  $\mu\text{m}$  glass slide after separation of the bonded CNT array, and c) SEM image of CNT array bonded to the 2.5  $\mu\text{m}$  thin-film of glass evaporated on a silicon wafer.

We have studied the chemistry of the bonding mechanism in greater detail through preliminary analyses of X-ray photoelectron spectra. The results indicate the presence of sodium on the CNT surface after removal from the glass slide surface subsequent to bonding, but no sodium was present before bonding. An increase in sodium concentration is also observed on the glass surface which faced the CNT array during bonding, indicating that sodium ions have migrated toward the CNT free tips.

### Thermal Contact Resistance Results

In this section, we compare the thermal performance before and after *in situ* bonding for typical CNT array interface samples. Figure 6 demonstrates the reduction of contact resistance upon bonding at a fixed applied pressure of 0.17 MPa on the interface for one such sample. The temperature difference at the unbonded interface is 32.8°C at 0.17 MPa pressure (solid line). *In situ* bonding is then carried out without disturbing any of the contacting surfaces at 0.17

MPa and 80 V. The temperature difference is reduced by 8.4% to 30.0°C (dashed line). Since no contact geometries were changed, this reduction in the temperature drop is attributed to the success of the bonding process and the subsequent enhanced thermal interface conductance.

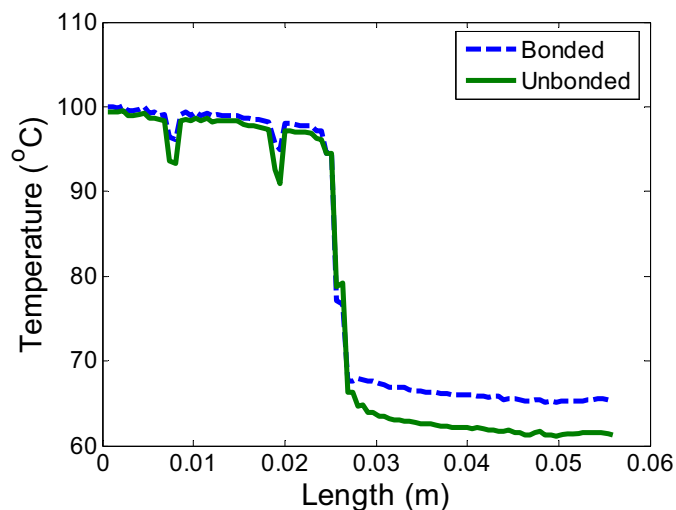


Fig. 6. Temperature profiles in the copper bus bars and linear curve fits for a CNT sandwich sample with 0.17 MPa applied pressure before and after bonding.

To understand the bonding process more completely, we perform a cyclic study of the variation of interface resistance with pressure and bonding on another typical CNT array interface sample. Figure 7 (dashed line) was obtained from a control experiment with a bare silicon wafer contacting the copper bars of the calorimeter. The value of the bare Si-Cu interface resistance is seen to reduce with pressure as expected, due to better contact.

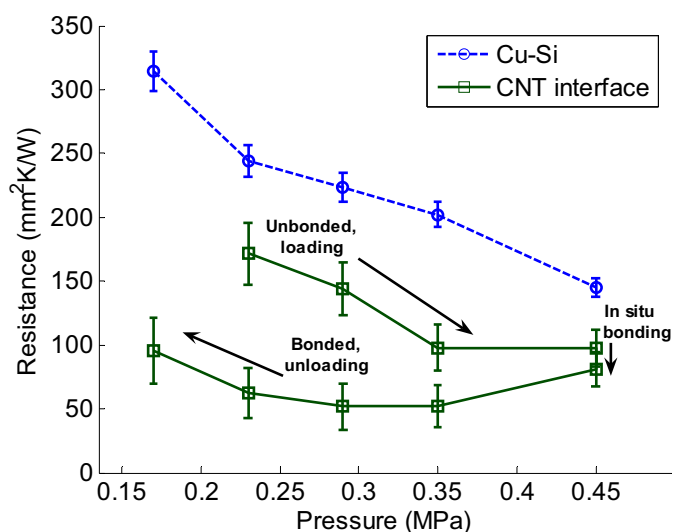


Fig. 7. CNT array to 2.5  $\mu\text{m}$  glass surface interface resistances and silicon-copper bar control interface resistances as a function of pressure.

A CNT array sandwich was then carefully placed between the copper bars, and an initial pressure of 0.23 MPa was applied. The pressure was then increased up to 0.45 MPa

and the CNT array was then bonded to the glass thin film at 0.45 MPa. Subsequently, the bonded interface was unloaded to a pressure of 0.17 MPa.

The resistance of the CNT array interface (solid line, Figure 7) is seen to decrease with pressure, as expected, from 172 mm<sup>2</sup>K/W at 0.23 MPa to 97 mm<sup>2</sup>K/W at 0.45 MPa. The interface is then bonded *in situ* at 0.45 MPa for 30 minutes at 80 V, and the thermal resistance is reduced by 17%, from 97 mm<sup>2</sup>K/W to 80 mm<sup>2</sup>K/W, due to the bonding process. Another important trend is that the resistance for the bonded interface is consistently less than that of the unbonded interface at lower pressures (Table 1). This reduction is in fact as high as 64% at pressures of 0.29 MPa and 0.23 MPa. At 0.45 MPa, the 17% reduction is also significant, because the resistance is already moderately low at the highest pressure studied. However, the decrease in resistance with decreasing pressure from 0.45 MPa to 0.35 MPa is yet to be understood fully. Overall, the reduction in the thermal resistance at the lower pressures is most beneficial from an application point of view.

The foregoing results indicate that the bonding process produces a favorable and significant change in thermal interface resistance. We note, however, that the magnitudes of these resistances are generally larger than those reported by Cola *et al.* [13] and Xu *et al.* [15]. We postulate that the longer CNT lengths (35 μm) and the presence of the extra glass layer in the present study were contributing factors to this difference and these issues are the subjects of ongoing study.

Table 1. Reduction in interface resistance due to bonding of CNTs.

Pressure (MPa)	0.23	0.29	0.35	0.45
Reduction in resistance	64%	64%	52%	17%

### CONCLUSIONS

We have demonstrated a new method to bond carbon nanotube arrays to glass. The motivation was to decrease the total interface resistance in a carbon nanotube array-based thermal interface material by reducing the dominant CNT free tip-to-contacting surface resistance. We have shown that bonding of the CNT tips to the glass surface is a chemical process, and that the adhesion force compares favorably to values in literature for other similar interfaces. Reductions in the interface resistance as large as 64% are observed at the interface due to the bonding process. In ongoing work, we are investigating the optimization of CNT length and bonding parameters to achieve lower resistances. Another parameter of interest is replacement of glass with conductors possessing suitable mobile alkali ions. The bonding process developed in this study will enable the use of CNTs close to their predicted potential in electronics cooling solutions and several other applications.

### ACKNOWLEDGEMENTS

The authors thank Baratunde Cola, Himanshu Mishra and Dr. Placidus Amama for help with the experiments and for stimulating discussions. We also gratefully acknowledge funding for this work from the NSF Cooling Technologies Research Center at Purdue University.

### REFERENCES

- [1] R. Mahajan, C. Chiu and G. Chrysler, "Cooling a microprocessor chip," Proceedings of the IEEE, Vol. 94, No. 8, pp. 1476-1486, 2006.
- [2] D. D. L. Chung, "Thermal interface materials," Journal of Materials Engineering and Performance, Vol. 10, pp.56-59, 2000.
- [3] R. Prasher, "Thermal interface materials: Historical perspective, status, and future directions," Proceedings of the IEEE, Vol. 94, No. 8, pp 1571-1586, 2006.
- [4] M. G. Dresselhaus, G. Dresselhaus and A. Jorio, "Unusual properties and structure of carbon nanotubes," Annual Review of Materials Research, Vol. 34, pp. 247-278, 2004.
- [5] S. Berber, Y. -K. Kwon and D. Tomaneck, "Unusually high thermal conductivity of carbon nanotubes," Physical Review Letters, Vol. 84 No. 20, pp. 4613-4616, 2000.
- [6] P. Kim, L. Shi, A. Majumdar and P. L. McEuen, "Thermal transport measurements of individual multiwalled nanotubes," Physical Review Letters, pp. 215502/1-215502/4, Vol. 87, 2001.
- [7] Y. Zhao *et al.*, "Interfacial energy and strength of multiwalled-carbon-nanotube-based dry adhesive," Journal of Vacuum Science and Technology B Vol. 24 No. 1, pp. 331-335, 2006.
- [8] S. T. Huxtable *et al.*, "Interfacial heat flow in carbon nanotube suspensions," Nature Materials, Vol. 2, pp. 731-734, 2003.
- [9] S. Shenogin, L. Xue, R. Ozisik, P. Keblinski and D.G. Cahill, "Role of thermal boundary resistance on the heat flow in carbon-nanotube composites," Journal of Applied Physics, Vol. 95 No. 12, pp. 8136-8144, 2004.
- [10] A. Javey, J. Guo, Q. Wang, M. Lundstrom and H. Dai, "Ballistic carbon nanotube transistors," Nature Vol. 424, pp. 654-657, 2003.
- [11] M. Nihei, M. Horibe, A. Kawabata and Y. Awano, "Carbon nanotube vias for future LSI interconnects," Proceedings of IEEE Interconnect Technology Conference, pp. 251-253, 2004.
- [12] J. Tersoff, "Contact resistance of carbon nanotubes," Applied Physics Letters, Vol. 74, pp. 2122-2124, 1999.

---

[13] B. Cola *et al.*, “Photoacoustic characterization of carbon nanotube array thermal interfaces,” *Journal of Applied Physics*, Vol. 101, pp. 054313/1-054313/9, 2007.

[14] R. Prasher, “Predicting the thermal resistance of nanosized constrictions,” *Nano Letters*, Vol. 5, No. 11, pp. 2155-2159, 2005.

[15] J. Xu and T. S. Fisher, “Enhanced thermal contact conductance using carbon nanotube array interfaces,” *IEEE Transactions on Components Packaging Technologies*, Vol. 29, pp. 261-267, 2006.

[16] W. H. Ko, J. T. Suminto and G. J. Yeh, “Bonding techniques for microsystems,” *Micromachining and Micropackaging of Transducers*, pp. 45-56, Elsevier, Amsterdam, 1985.

[17] B. Schmidt *et al.*, “In situ investigation of ion drift processes in glass during anodic bonding,” *Sensors and Actuators A*, Vol. 67, pp. 191-198, 1998.

[18] P. Yu, “The anodic bonding between  $K_4$  glass and Si,” *Materials Letters*, Vol. 59, pp. 2492-2495, 2005.

[19] A. Cupolillo, C. Giallombardo and L. Papagno “Electronic properties of alkali-metal intercalated single walled carbon nanotubes”, *Surface Science*, Vol. 601, No. 13, pp. 2828-2831, 2007.

[20] W. B. Choi *et al.*, “Experimental analysis of the anodic bonding with an evaporated glass layer,” *Journal of Micromechanics and Microengineering*, Vol. 7, pp. 316–322, 1997.

[21] J. P. Holman, *Experimental Methods for Engineers*, 6th ed., New York: McGraw-Hill, pp. 49–62, 1994.